Journal of Insect Physiology 54 (2008) 1467–1478

Contents lists available at ScienceDirect

Journal of Insect Physiology

journal homepage: www.elsevier.com/locate/jinsphys

Correlations of cibarial muscle activities of *Homalodisca* spp. sharpshooters (Hemiptera: Cicadellidae) with EPG ingestion waveform and excretion

Sebastien Dugravot [a,1], Elaine A. Backus [b,3,*], Brendon J. Reardon [a,2,3], Thomas A. Miller [a]

[a] *Department of Entomology, University of California, Riverside, CA 92521, USA*
[b] *USDA Agricultural Research Service, San Joaquin Valley Agricultural Sciences Center, 9611 So. Riverbend Avenue, Parlier, CA 93648, USA*

ARTICLE INFO

Article history:
Received 31 December 2006
Received in revised form 2 May 2008
Accepted 7 May 2008

Keywords:
Electrical penetration graph
Electronic monitoring
Xylella fastidiosa
Pierce's Disease
Feeding

ABSTRACT

Fluid flow into and out of the stylets of xylem-ingesting sharpshooters (Hemiptera: Cicadellidae: Cicadellinae) is powered by muscles of the cibarial pump. Such fluid flow is crucial for transmission of *Xylella fastidiosa*, the Pierce's Disease bacterium, yet has not been rigorously studied via electrical penetration graph (EPG) technology. We correlated EPG waveforms with electromyographically (EMG) recorded muscle potentials from the cibarial dilator muscles, which power the piston-like cibarial diaphragm. There was a 1:1 correspondence of each cycle of cibarial muscle contraction/relaxation with each plateau of EPG waveform C. Results definitively showed that the C waveform represents active ingestion, i.e. fluid flow is propelled by cibarial muscle contraction. Moreover, each C waveform episode represents muscular diaphragm uplift, probably combined with a "bounce" from cuticular elasticity, to provide the suction that pulls fluid into the stylets. Fine structure of the EPG ingestion waveform represents directionality of fluid flow, supporting the primary role of streaming potentials as the electrical origin of the C waveform. Rhythmic bouts of cibarial pumping were generally correlated with sustained production of excretory droplets. However, neither the onset nor cessation of ingestion was correlated with onset or cessation of excretion, respectively. Volume of excreta is an inexact measure of ingestion. Implications for using EPG to understand the mechanism of *X. fastidiosa* transmission are discussed.

Published by Elsevier Ltd.

1. Introduction

Fluid flow into and out of the stylets of piercing-sucking hemipterans is mediated by the cibarial dilator muscles that power the piston-like cibarial pump (Snodgrass, 1935; Smith, 1985), plus the precibarial valve and its muscle (Backus and McLean, 1982; McLean and Kinsey, 1984). This portion of the hemipteran anterior foregut is delimited by the apposition of the epi- and hypopharyngeal plates. The cuticular indentations in these two plates together form the precibarium, a narrow channel immediately after the stylet food canal, and the cibarium, the food pump (Backus and McLean, 1982, 1983).

In leafhoppers (Family Cicadellidae) and other members of Suborder Auchenorrhyncha, the precibarium and cibarium have a funnel-like shape, with the precibarium (the stem of the funnel) markedly narrower than the wider cibarium (the bowl of the funnel). The large cibarial dilator muscles originate on the interior of the facial cuticle of the clypeus in these insects, and insert on a broad, flat, sulcus-like apodeme in the lid, or diaphragm, of the cibarium (Snodgrass, 1935; Backus and McLean, 1983). The precibarium is lined with chemosensory papillae, separated into two functional groups by a precibarial valve that is housed in a grooved and recessed, basin-like structure (the epipharyngeal basin) and closes against a protuberance in the hypopharynx. The precibarial valve is powered by a tiny muscle, the precibarial valve muscle, whose innervation and operation is separate from those of the cibarial dilator muscles (Backus and McLean, 1982; Backus and Dugravot, unpublished data). However, the structure of the epipharyngeal basin also suggests that a strong, backward flow of fluid from the cibarium could physically force the valve closed (Backus and McLean, 1982), allowing it to function as a pressure-sensitive check valve to aid swallowing. In aphids and other

* Corresponding author. Tel.: +1 559 596 2925.
E-mail addresses: sebastien.dugravot@univ-rennes1.fr (S. Dugravot), elaine.backus@ars.usda.gov (E.A. Backus), brendon.reardon@aphis.usda.gov (B.J. Reardon), thomas.miller@ucr.edu (T.A. Miller).
[1] Present address: EA3193 Equipe d'Ecobiologie des Insectes parasitoïdes, Université de Rennes 1, Campus de Beaulieu, 263 Av du général Leclerc, 35042 Rennes, France.
[2] Present address: USDA Animal and Plant Health Inspection Service, 350 Corporae Blvd., Robbinsville, NJ 08691, USA.
[3] Mention of trade names or commercial products in this article is solely for the purpose of providing specific information and does not imply recommendation or endorsement by the U.S. Department of Agriculture.

0022-1910/$ – see front matter. Published by Elsevier Ltd.
doi:10.1016/j.jinsphys.2008.05.008

members of the Suborder Sternorrhyncha, the precibarium and cibarium are tubular, with very little difference in size or orientation between the two sections. However, the two parts can be distinguished by the origins of the precibarial valve and cibarial dilator muscles (McLean and Kinsey, 1984).

Identifying the mechanism of transmission of plant pathogens by certain hemipteran vectors relies, in part, on understanding: (1) the directionality and timing of fluid flow through the foregut, (2) when the cibarial pump and precibarial valve are activated, and (3) through which chambers the fluid moves. This is especially true for sharpshooter (Cicadellidae: Cicadellinae) vectors of the xylem-limited bacterium, *Xylella fastidiosa* Wells, causative agent of Pierce's Disease of grape, because it is thought that inoculation occurs via outward fluid flow carrying bacteria from colonies in the precibarium and/or cibarium (Almeida and Purcell, 2006). Although a variety of methods have been used to study sharpshooter ingestion (Dolezai et al., 2004), electrical penetration graph (EPG) monitoring of insect feeding remains the most rigorous tool to understand the microdynamics of fluid flow.

EPG has revolutionized the study of hemipteran feeding in the last 45 years (Walker and Backus, 2000). Waveforms are produced when a gold-wire-tethered insect is made part of a circuit with an electrified plant. EPG waveforms can be very precisely correlated with stylet tip locations, stylet activities, and fluid flow by using a range of methods, including correlation with electromyography (EMG) of muscle movements (Tjallingii, 1988). Previous studies of sharpshooter EPG waveforms have revealed great detail about these insects' stylet penetration, or probing (Backus et al., 2005; Joost et al., 2006). Probing comprises three phases: (1) pathway phase, in which stylets penetrate (probe) shallow plant tissues on the way to the ingestion tissue (for sharpshooters, usually xylem), and composed of specific behaviors for salivary sheath construction, tasting, and stylet movements, (2) ingestion phase, usually in the xylem, and (3) interruption phase, in which ingestion ceases momentarily for salivation, tasting or probing to a different ingestion cell (Joost et al., 2006).

Questions about sharpshooter stylet penetration remain, and impede our complete understanding of *X. fastidiosa* transmission, i.e. acquisition and inoculation. First, in relation to EPG signals, can waveform fine structure provide information about specific muscle movements, or rate and directionality of fluid flow (perhaps via streaming potentials [Walker, 2000]) during stylet penetration? If so, what further mechanisms of *X. fastidiosa* transmission could be better explained via EPG analysis? Second, many scientists studying these insects use quantification of excretory droplets as a proxy for ingestion (Anderson et al., 1989; Dolezai et al., 2004), but exactly how accurate a proxy is excretion?

To answer these questions, we studied the smoke tree sharpshooter, *Homalodisca liturata* Ball (Burks and Redak, 2003; formerly *H. lacerta*) a native California sharpshooter that is a closely related, congeneric species to the glassy-winged sharpshooter, *Homalodisca vitripennis* (Germar) (Takiya et al., 2006; formerly *H. coagulata*), an exotic, invasive species recently introduced to California from Texas (de Leon et al., 2004). Concurrent work (Backus and Bennett, unpublished data) has shown that EPG waveforms of *H. liturata*, also a vector of *X. fastidiosa*, are virtually identical to those of the quarantined *H. vitripennis*.

The objective of this study was to test the hypotheses that: (1) cibarial dilator muscle movements are correlated with fine structure of the EPG ingestion waveform (C), the waveform most likely to represent cibarial pumping (Backus et al., 2005; Joost et al., 2006), and (2) excretory droplet production is correlated with cibarial pumping-mediated, active ingestion.

2. Methods and materials

2.1. Insect rearing

H. liturata were greenhouse-reared to adulthood on a mixture of healthy cowpea, *Vigna unguiculata* (L.), sorghum, *Sorghum bicolor* (L.) and sweet basil, *Ocimum basilicum* (L.) plants in the same cage, at the USDA, Agricultural Research Service, San Joaquin Valley Agricultural Sciences Center in Parlier, CA, USA. Artificial lighting was used to augment natural lighting for a photoperiod of 16:8 (L:D). The rearing of *H. liturata* was initiated from insects collected on jojoba, *Simmondsia chinensis* (Schneid), at Agricultural Operations, University of California, Riverside, CA, USA. Insects used in this study were a mixture of young and old adults, both females and males. Their innoculativity status of *X. fastidiosa* was unknown.

2.2. EPG recordings

After being briefly immobilized with CO_2, test sharpshooters were tethered with a semi-thin gold wire, 63.5 μm diameter (sold as 0.0025 in.; Sigmund Cohn, Mount Vernon, NY) and 1.5 cm long, glued to the insect's mesonotum via conductive silver paint (Ladd Research Industries, Burlington VT; *N*-butyl acetate solvent). The sharpshooters were dangled by their wires, without tarsi touching a surface, for a 2 h starvation period. The sharpshooter and a test cowpea plant were connected together in an electrical circuit through the gold wire and another electrode, a copper wire, inserted into the soil of the potted plant (Fig. 1a).

When the sharpshooter started probing, an electrical circuit was completed through an AC–DC 4-channel monitor (designed and built by W.H. Bennett, University of Missouri, retired, and E.A.B.). Current passing through the circuit was displayed as time-varying voltage signals, producing waveforms. The new AC–DC 4-channel monitor allows the user to choose settings to replicate either a classical AC EPG monitor or a classical DC EPG monitor (Backus et al., 2000), or to blend the capabilities of each. For most of our recordings, we used classical DC monitor signal processing, i.e. 10^9 (Giga) Ω input impedance (Ri) and no applied (substrate) voltage (i.e. neither AC nor DC excitation to the plant). For sharpshooters, this results in signals whose electrical origins are exclusively electromotive force (emf) (Backus, unpublished data). This setting was originally chosen because it provided slight enhancement of our signal of interest (waveform C), because its electrical origin is predominantly emf (Walker, 2000; Backus and Bennett, unpublished data; also see Section 4). However, once studies were half-completed, we switched to 10^6 Ω Ri and a slight,

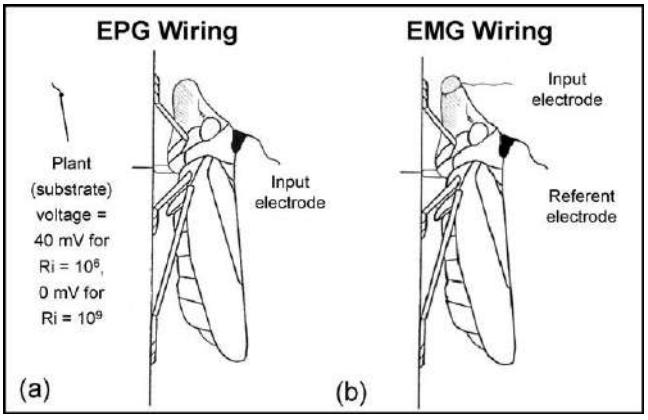

Fig. 1. Comparison of the electrode wiring for (a) electrical penetration graph (EPG) recordings and (b) electromyography (EMG) recordings. See text for discussion.

40 mV substrate voltage, so that EPG signals portrayed in the figures were more similar to our previously published sharpshooter waveforms (Backus et al., 2005). In this manner, we were able to test our cibarial pumping correlation for both AC- and DC-type EPG waveforms.

Waveforms were digitally acquired at a sample rate of 100 Hz., using a WinDaq DI-720 analog-to-digital converter and displayed with WinDaq Pro+ software (DATAQ Instruments, Akron, OH) on a Dell PC computer. Each probe ranged from 15 min to 1 h per insect. Recordings were made throughout the day, under artificial light at approximately 25 °C.

2.3. EMG recordings

When no substrate voltage plus high input impedance with the DC signal processing channel are used, the AC–DC monitor can be used in a manner similar to an electromyograph. We therefore used the same AC–DC monitor to record EMG waveforms, sampled at 100 Hz, with no substrate voltage, filtering or rectification, and 10^9 Ω Ri. Preliminary recordings were made at 2000 samples per second, for most accurate representation of any high-frequency signals that might be present. However, the mean repetition rate was the same at both 2000 Hz. (34.6 ± 5.3 Hz [std. dev.; n = 15]) and 100 Hz (34.2 ± 3.6 Hz [std. dev.; n = 15]). Thus, the 100 Hz sample rate was sufficient to capture the unusually low-frequency spike bursts of these insects. In addition, spike burst durations were not significantly different between recordings at 2000 vs. 100 Hz ($P > 0.600$). Therefore, 100 Hz was used for experiments, to reduce sizes of data files. Waveforms were acquired with the same WinDaq hardware, software and computer as for EPG.

The single referent electrode was a gold wire (similar size as above, for EPG) glued to the insect's mesonotum using the method described above (Fig. 1b). Immediately after the first wiring, the insect was vacuum-immobilized on its dorsum. The input electrode, a second gold wire (similar size), then was inserted shallowly into the cibarial dilator muscles at the anterior end of the insect's face, through a small aperture in the cuticle that had previously been punctured with a minuten pin. An attempt was made to minimally disturb the underlying tissues, however, some wounding was inevitable. The aperture was made in the pigmented areas on the facial cuticle that correspond to the cibarial muscle origins, according to previous morphological studies (Backus and McLean, 1983). The gold wire's position inside the head was then secured by application of softened, partially melted dental wax (Longs Drug Corp., Walnut Creek, CA, USA) around the aperture and the crown of the head (Fig. 1b). Accurate location of the wire embedded in these muscles was verified after recording by insect head dissection and observation under a stereomicroscope.

After wiring, the sharpshooters were dangled by the referent electrode in a manner similar to above for EPG, for a 2 h starvation period. Then (in the experimental EMG treatment, but not the EPG control treatments) the input electrode was connected to the input of the head stage amplifier and the referent electrode was connected to the substrate voltage plug. Time of day and temperature for recordings were as above. Insects were recorded for about 1 h after onset of probing, or until stylet probing ceased. A new cowpea plant was used for each new individual.

2.4. Tests of correlation between EMG and EPG

For the best correlation, attempts were made to record EPG and EMG waveforms simultaneously from the same insect, each displayed on its own separate monitor channel yet time-synchronized. Wires were placed on the mesonotum and in the cibarial dilator muscles of the same insect (as described above), and then were plugged into the monitor in all possible circuit combinations. Unfortunately, none gave the desired results. Instead, EMG and EPG waveforms were blended together in each of the recording channels, not separated. Also, because the repetition rate of the EMG spike bursts was unusually low, high pass filtering could not be used to separate the blended signals.

In absence of a method to directly correlate EMG and EPG waveforms, we began recording one type of signal at a time from each individual insect, and sought an external correlate that could bridge the EPG and EMG data. To search for such an indirect means of correlation, EMG and EPG recordings were time-synchronized with videography of the insect's body posture and behavior. At the outset of experimentation, we hypothesized that excretory droplet production might provide a correlate. Upon viewing of the first half of videos recorded (most of the EMG and EPG only treatments) we observed that light reflectance on the moving cibarial diaphragm was visible (see Section 2.7.3). Thus, in the end, we tested whether videos of either: (1) excretory droplet production during ingestion, or (2) cibarial diaphragm movements could be separately correlated with either or both EPG or EMG waveforms, to provide an inferential bridge between the two.

2.5. Treatments and access/recording times

EPG recordings also were used for wound control insects, to test the effects of cibarial muscle wounding and electrification. It was necessary to use EPG for these controls instead of EMG, because EMG signals could only be obtained by electrifying the muscle-inserted wire. Thus, a total of four electrical treatments were used: (1) EPG only (i.e. no head-puncture; Fig. 1a), (2) EPG with head-puncture, (3) EPG with head-puncture, wire inserted, but not electrified (termed head-punctured–wired), and (4) EMG (i.e. head-punctured with wire inserted and electrified; Fig. 1b).

Twenty-nine insects were prepared and recorded for the EMG treatment (i.e. recording cibarial spike bursts), and all were partially to fully successful. Ten to 12 insects each were successfully recorded for the three EPG treatments, i.e. EPG only, EPG head-punctured, and EPG head-punctured–wired. The seven best recordings (i.e. the longest feeding durations with wires intact) from each of the four treatments were chosen for quantitative, statistical analysis.

After preliminary analysis of results from these four treatments, concerns arose that differences in excretory droplet output and feeding measurements (described in Section 3.2) might be related to excessively variable access times (i.e. the durations of the insect sitting on the plant) or recording times (i.e. the portion of access time when recordings were made). Therefore, three parameters were measured after recording was completed, and were statistically analyzed. They were: (1) access time on the plant, (2) duration of EMG or EPG-recorded probing, and (3) duration of video-recorded probing. Access time was always longer than either EMG/EPG recordings or video recordings. Nonetheless, durations of these parameters among the four treatments were not significantly different within each measured parameter (see Section 2.7.1). Therefore, variation in results was not due to variable access or recording times.

2.6. Video acquisition of insect behavior and synchronization with EPG or EMG waveforms

Videography of the whole body of all insects was carried out during stylet penetration using a Leica MZ12.5 stereomicroscope (Leica Microsystems Ltd., Jena, Germany), with a magnification range of 8–10×. A side-view image of each EPG- or EMG-recorded

sharpshooter feeding on the plant was recorded with a CCD camera (JK-TU52h Toshiba Corporation, Tokyo, Japan) connected to the stereomicroscope. A fiber optic 'cold light' (Schott 150H Universal, Schott Fiberoptik, Germany) was used as the light source. The video signal from the CCD camera was fed into a Dell Optiplex computer (Dell Corporation, Austin, TX, USA) through a video card (Canopus MVR1000, Canopus Corporation, San Jose, CA, USA) and digitized at 30 frames per second with MediaCruise software (Canopus Corporation, San Jose, CA) in an mpeg-2 format.

In order to accurately synchronize the videographic, EMG and EPG signals for later viewing with The Observer software (see Section 2.7, below), a synchronizing device (Video Synchronizer, patent pending) was designed and built by W.H. Bennett, University of Missouri, retired. The device had a small, red light-emitting diode (LED) light at the end of a thin cable. The light was positioned near the insect, in view of the videocamera. The cable was attached to an electrical device that was then plugged into the input of the AC–DC EPG monitor. Upon depression, a button on the Synchronizer would simultaneously elicit a series of red light flashes (3.3 Hz, or one every 300 ms) as well as spikes on the EPG trace (Fig. 2a, top waveform, "Event marker"). A series of light flashes and spikes was made at the end of each individual insect's recording.

2.7. Waveform and video analysis

The recorded videos and EMG or EPG waveforms for each insect tested were transferred into The Observer software (Noldus Information Technology, Wageningen, The Netherlands). Both videos and waveforms were then accurately time-synchronized in The Observer by associating the synchronizing red flashes with the spikes previously recorded. The program then linked videos and waveforms running at the same time and enabled coordinated coding (measurement) of files.

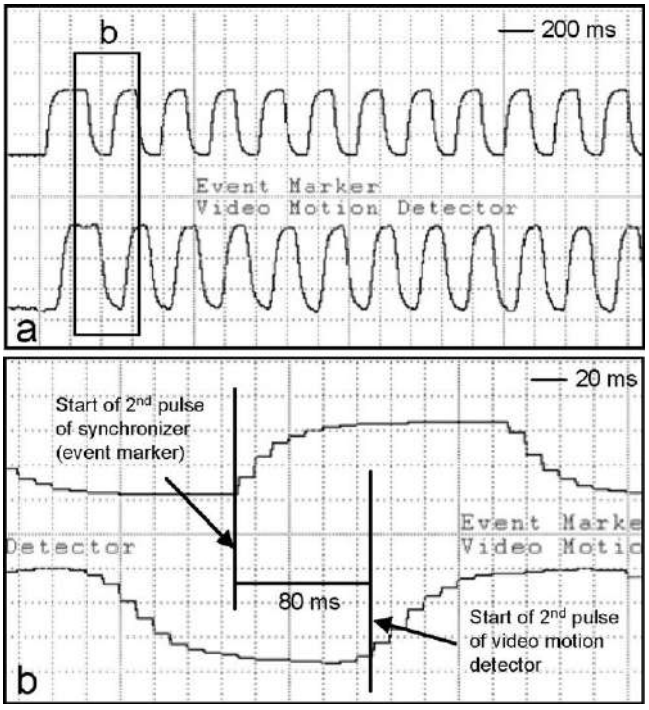

Fig. 2. Waveforms transduced from the light flashes of the Synchronizer. (a) Original waveform from the Synchronizer (top channel, user annotation Event Marker) compared with the secondary waveform from transduction of the red light flashes by the video motion detector (VMD; bottom channel, user annotation is video motion detector). The box labeled b is expanded in part b. (b) Expanded portion from part a, showing the 80 ms time lag between the original waveform (top) and the second VMD waveform (bottom). WinDaq gain 4× in both views.

2.7.1. Quantitative analysis of waveform episodes and excretory droplets

Each droplet excreted during the video-captured probing process was coded in The Observer. Simultaneously, we also coded all individual plateaus and valleys during the C waveform, i.e. the ingestion waveform (Almeida and Backus, 2004; Backus et al., 2005; Joost et al., 2006) recorded by EPG, or individual spike bursts recorded by EMG. Hereafter, these will be collectively termed "waveform episodes." Many episodes were also manually counted. Seven different excretion parameters were averaged for each insect, then averaged by treatment, for all four treatments: (1) time to the first droplet in a sustained train of droplets excreted after the beginning of a bout of waveform episodes, (2) number of waveform episodes occurring before the first droplet, (3) number of waveform episodes, (4) number of excretory droplets, (5) number of waveform episodes per droplet, as calculated by dividing the number of waveform episodes by the number of droplets, (6) duration of the ingestion phase (i.e. each bout of waveform episodes, including brief interruptions), and (7) excretion rate (i.e. number of droplets per second), as calculated by dividing the number of droplets excreted by the duration of ingestion phase for each insect.

Durations of representative episodes (20% each, randomly chosen) of the EMG cibarial spike bursts and EPG C plateaus were measured and statistically compared, using the parameters in Backus et al. (2007). Five of the previously chosen seven insects that were EMG-recorded produced easily-measured, noise-free recordings; three of these recordings had signals categorized as spike bursts (termed section p, for potential) plus sections m (for middle) and b (for baseline) (see description under Section 3.1.2). The other two recordings' baselines were too noisy to delimit section m from b, therefore these recordings only had p and b sections. All seven previously chosen insects that were EPG-recorded had measurable recordings. Combinations of EMG section durations were statistically compared with the EPG episode durations.

2.7.2. Statistical analyses

Repeated-measures analysis of variance (restricted maximum likelihood estimation; REML-ANOVA) (PROC MIXED, SAS Institute, 2001) was used for all comparisons. The dependent variable of the models was the mean frequency or duration, and the fixed effect was the treatment (i.e. EMG, EPG only, etc.). The random effect in the models was the interaction of insect subject and treatment. Treatment means were separated using the least significant difference test (LSMEANS option with the Tukey–Kramer adjustment), and the degrees of freedom were estimated using the Satterthwaithe's approximation (SAS Institute, 2001). The REML-ANOVA models' assumptions were assessed with residual and normal plots. At each level of treatment, all data met the model assumptions of ANOVA, i.e. homoscedasticity and normality (Fry, 1993; Ott and Longnecker, 2001). Thus, ANOVA was the most powerful statistical test to use for this data. Differences were considered significant at $\alpha = 0.05$.

2.7.3. Qualitative analysis of waveforms and cibarial diaphragm movements

Upon examination of previously recorded videos of probing insects subjected to the EPG-only treatment, we observed that the lift and release of the cibarial diaphragm by the cibarial dilator muscles in the insect head were visible as the degree of light flickering in the videos of sharpshooter feeding (Fig. 3). This

Fig. 3. Still image of a smoke tree sharpshooter captured from a video recording of feeding while simultaneously EPG-recorded (wire on dorsum). White circles represent the area delimited by the VMD's detection window, shown at both the cibarium (upper left circle) to detect cibarial diaphragm movements, and at the anal ligulae (lower circle) to detect excretory droplets. Image was captured at the instant of expulsion of a droplet (line at lower right). The upper right-hand circles show representative examples of the darkest (top) and brightest (bottom) views of the cibarium. Magnification 10×.

apparently was possible because this species is quite large for a leafhopper (9 mm body length), the cuticle is somewhat transparent, and the area of the anteclypeus was backlit during recording. The reflection of light inside the cibarium usually became brighter as the diaphragm was lifted (perhaps because the cibarium filled with transparent xylem fluid), and darker as the diaphragm fell (when the cibarium filled with the diaphragm). However, in some cases (see figures and Section 3.3), light was reflected in an opposite manner, so that the cibarium became darker as the diaphragm rose. This may have been due to the insect's position in relation to the backlight. In all cases, however, the flickering change in light intensity was obvious, and appeared to be correlated with C plateaus.

2.7.4. Video motion detector

To provide the most rigorous correlation and to provide graphical representations for figures, the motions of droplet propulsion or diaphragm movements were converted into waveforms during recordings for the last half of the project, i.e. EMG ($n = 2$), EPG only ($n = 2$), EPG-punctured ($n = 7$), and EPG-punctured–wired ($n = 7$). A video motion detector (VMD) device (patent pending) was designed and built by W.H. Bennett, (University of Missouri, retired). It consists of two photodiodes and an amplifier that act as a light-to-voltage converter responding to light with wavelengths of 320–1050 nm. Two rubber grommets of 8 mm diameter (hereafter termed the detection window), each housing one photodiode, sent each of their signals to an amplifier that in turn was attached to the input of the AC–DC EPG monitor so that the photodiode signals could each be displayed on a separate channel of the output. Each detection window was tightly held onto the computer screen (via clamping to a stationary ring stand) over the area of interest while the recording video was being displayed on the screen. Given the relative size of the insect on the screen, the 8 mm-area of the detection window was large enough to cover the entire area of interest (Fig. 3). The insects always sat very still on the plant during ingestion, so that the area of interest almost never moved out of range of the photodiode. However, if the insect (rarely) moved, either a slight drift or abrupt offset of the signal occurred over time; neither disturbed the basic information of the signal. The signal output from the VMD was a positive voltage whose amplitude varied directly with brightness. Thus, the peak of the waveform indicated the brightest light, i.e. usually when the cibarium was most open (Fig. 3, circles in the upper right), or a droplet was expelled. Flicking of the anal ligulae and subsequent droplet expulsion produced a flash of light (Fig. 3, lower circle). The resulting waveforms were simultaneously recorded and co-synchronized via three channels of the AC–DC monitor. Channel 1 always showed either EMG or EPG waveforms, channel 2 showed the waveform for cibarial diaphragm movements, and channel 3 showed the waveform for droplet expulsion (see remaining figures).

2.7.5. VMD synchronization lag

A slight time lag occurred between our VMD recordings and EMG/EPG recordings (Fig. 2b), caused by our post-EPG recording method for the VMD video-to-waveform conversion. As explained above, VMD figures were generated by recording of the VMD along with either the EPG or EMG signals. The cibarial diaphragm movements were displayed on the computer screen as video images, plus simultaneously recorded via EPG or EMG, which also were displayed in a separate window on the computer screen. The VMD's photodiode transduced light flashes from the computer screen into voltage signals that were sent secondarily to the second channel in the EPG monitor, which was then displayed in the WinDaq view, alongside the EPG/EMG channel. Thus, the VMD waveform was transduced temporally later than the EPG/EMG signal was produced, causing a reliably constant time lag. To provide an exact measure of this lag, we used the VMD to transduce light flashes of the Synchronizer into secondary waveforms, and compared the VMD waveform with the original Synchronizer waveform (Fig. 2b). The synchronization lag measured 80 ms, which was then used as a correction factor for the VMD figures.

3. Results

3.1. EPG and EMG waveform appearances

3.1.1. EPG waveforms

EPG signals at Ri $10^6\ \Omega$ were typical for sharpshooters feeding on plants, including all waveform types from pathway, ingestion and interruption phases (similar to Almeida and Backus, 2004; Backus et al., 2005). Waveforms recorded at Ri $10^6\ \Omega$ (in figures) were similar to those recorded at Ri $10^9\ \Omega$ (not shown), except that sometimes they were inverted (especially waveform C), and had slightly lower amplitude of emf-component waveforms such as C.

Waveform C was clearly present and correlatable at both Ri 10^6 and $10^9\ \Omega$. At Ri $10^6\ \Omega$, it consisted of a highly repetitive series of plateau-and-valley episodes whose fine structure was slightly variable from individual to individual (see figures below).

Waveform C at Ri $10^9\ \Omega$ was composed of similar plateaus (data not shown) with slightly deeper valleys between the plateaus and less variability in fine structure from individual-to-individual than at Ri $10^6\ \Omega$.

We recorded a total of 18,385 separate C episodes from the EPG-only treatment, 10,967 from the EPG head-punctured treatment, and 9583 from the EPG head-punctured–wired treatment; both of the latter were EPG controls for the EMG treatment.

3.1.2. Cibarial EMG muscle potentials

Cibarial spike bursts were recorded from preparations of cibarial muscles punctured, wired and electrified (i.e. EMG only), and undoubtedly represent muscle activities for the cibarial dilator muscles. We recorded 17,899 separate spike bursts from the EMG treatment. The appearance of cibarial spike bursts varied slightly from insect to insect, perhaps due to variable wire placement. However, several features were common to most (Fig. 4f). EMG episodes showed a spike burst of high amplitude followed by very low-amplitude, slightly noisy baseline that was divided into two sections (m and b; Fig. 4f, black arrows) by a single, short, negative-going spike in >80% of the episodes (Fig. 4e–g). Rarely, there would be more than one spike, if the cibarial diaphragm moved very slowly (Fig. 4b).

Video recording showed that bouts of cibarial spike bursts did not begin until several minutes after initial proboscis contact and the start of stylet penetration inside plant tissues. Timing of cibarial muscle potentials thus matched the timing of ingestion phase, which occurs after pathway phase (at the beginning of the probe), is completed.

3.2. Comparison of EPG and EMG waveforms using excretory droplets

Synchronization of EMG/EPG episodes with droplet expulsion, via both The Observer video analysis and VMD, showed no direct, 1:1

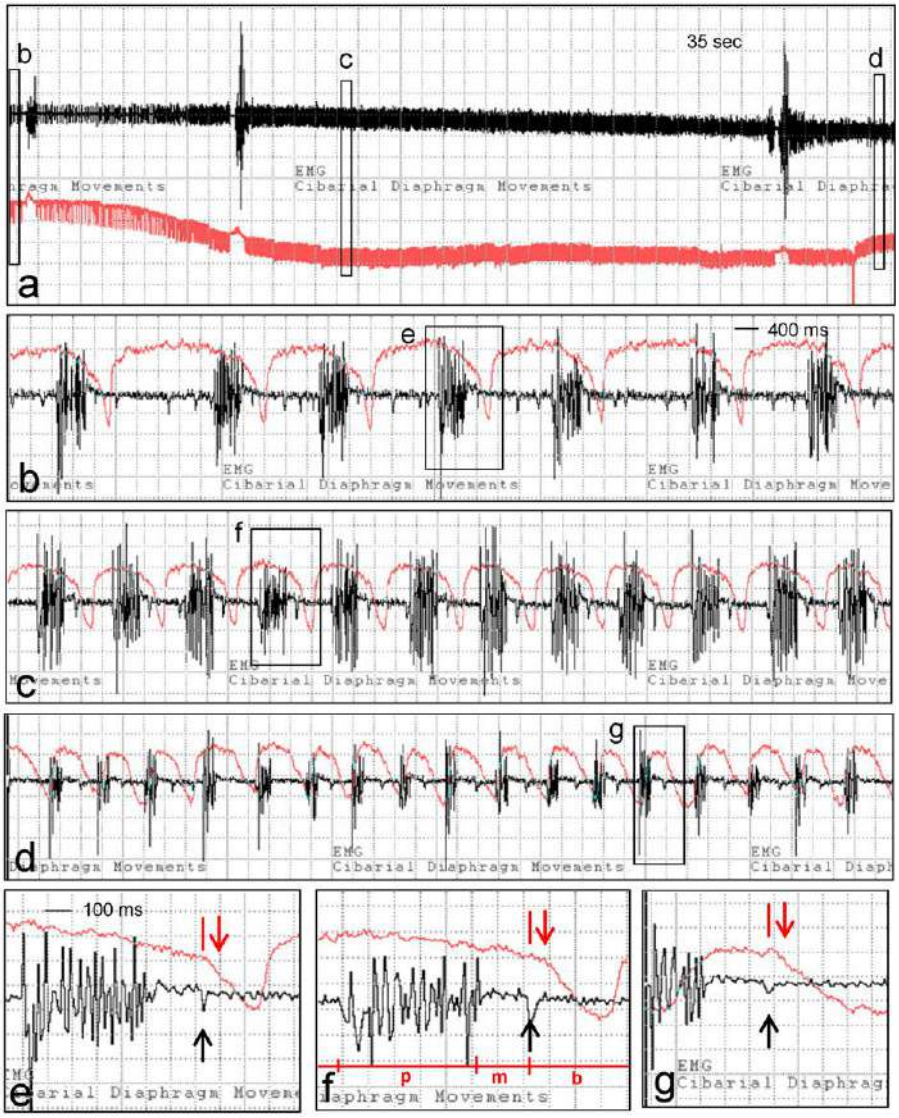

Fig. 4. EMG recordings of cibarial dilator muscle potentials with near-simultaneous VMD recording of cibarial diaphragm movements. (a) Compressed view of the many hundreds of spike bursts and cibarial pumps recorded in a short time; view begins at 117 s after the start of recording, ends at 1700 s. Upper channel (black) shows EMG spike bursts (user annotation same); lower channel (red) shows VMD waveform (user annotation cibarial diaphragm movements). The same color scheme for waveforms is repeated in other figure parts. Boxes b, c and d show the positions of waveform excerpts expanded in parts b, c and d. WinDaq gain 2×. (b–d) Amplified and expanded views of boxes b, c and d, respectively, shown in part a. Slow (0.35–0.5 Hz, measured), medium (0.7–0.85 Hz) and rapid (1–1.25 Hz) speed pumping, respectively. Boxes e, f, and g are the boxed excerpts in each, further expanded and labeled in parts e, f and g, respectively. WinDaq gain 16×. Time scale in part b applies to parts c and d also. (e–g) Amplified and expanded views of boxes e, f and g in parts b, c and d, respectively. Synchronizer lag indicated by red lines and arrows. The red arrow shows the red (VMD) waveform feature that should be moved back to the position of the red line. EMG waveform sections p, m and b are labeled in red at the bottom of box f. WinDaq gain 16×. Time scale in part e applies to parts f and g also.

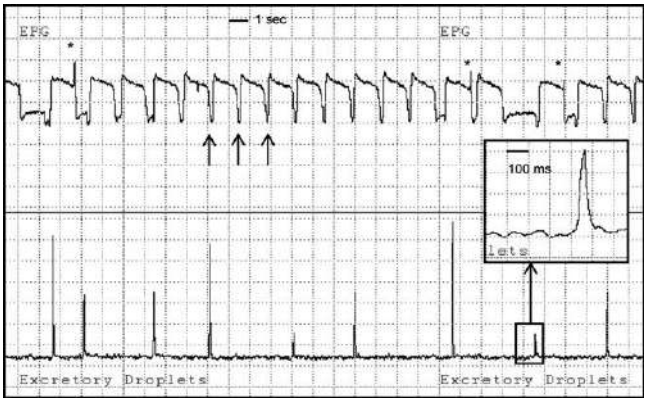

Fig. 5. EPG recordings (top channel, user annotation EPG) at Ri 10^6 Ω (see text) from a wired–punctured control insect, with near-simultaneous VMD recording of excretory droplet expulsion (bottom channel, user annotation Excretory Droplets). Inset box shows expanded view of one droplet waveform, to show that its base measures ~100 ms. EPG waveform displays medium-speed pumping (0.75 Hz), with complete depth of C plateau valley (example arrows). Thus, C valley depth is only lost at higher-speed pumping (see Fig. 6c and d). Occasional peaks on the end of the plateaus are indicated with asterisks. WinDaq gain 32× for both channels.

correlation for either EMG or EPG waveform with droplets (Fig. 5). In the VMD waveform, each droplet expulsion caused a rapid rise and fall of voltage (Fig. 5, lower channel). Voltage amplitude was variable, depending upon the brightness of the light flash, which presumably depended on the angle of the anal ligulae in relation to the videocamera at the instant of expulsion (Figs. 3 and 5). Frequency of droplet expulsion was often highly variable (Fig. 6), especially at the beginning of ingestion, but then usually settled down to a regular pattern of once every 2–5 cibarial diaphragm pumps, once ingestion became sustained. The duration of each individual droplet expulsion was about 0.1 s (100 ms) (Fig. 5).

Statistical analysis of the seven excretory droplet parameters also showed lack of correlation with EMG or EPG waveforms. However, excretion parameters were strongly affected by wounding, as revealed by the wire insertion controls (Table 1). As severity of physical wounding to the insect increased with treatment, ingestion time to first droplet was numerically (though not significantly) lengthened. EPG-only insects (i.e. with no head-puncture) had numerically the shortest time to first droplet, with EPG head-punctured slightly longer, EPG head-punctured–wired longer, and EMG (i.e. head-punctured–wired–electrified) the longest. When a two-sample test, comparing EPG only with EMG, was performed, ingestion time to first droplet became significantly shorter for EPG only compared with EMG (d.f. = 1; $F = 5.06$, $P = 0.0441$). Likewise, number of waveform episodes to first droplet was significantly different overall (d.f. = 3; $F = 6.57$, $P = 0.0021$). Pairwise comparisons showed significantly more episodes for EMG compared with EPG head-punctured ($P = 0.0028$), EPG head-punctured–wired ($P = 0.004$), and EPG only ($P = 0.007$). Two other parameters, overall number of episodes and duration of ingestion phase (per insect by treatment), were not significantly different among treatments. In contrast, the next two parameters were both significantly different between EPG only and any treatment that punctured the cuticle. For both overall number of droplets (d.f. = 3; $F = 5.71$, $P = 0.0054$), and number of droplets per second (excretion rate) (d.f. = 3; $F = 12.08$, $P = 0.0001$), overall ANOVA showed significant differences. Means for the two parameters were significantly greater for EPG only than for EPG head-punctured ($P = 0.0001$ and $P = 0.0052$, respectively), EPG head-punctured–wired ($P = 0.0001$ and $P = 0.007$, respectively), or EMG ($P = 0.0001$ and $P = 0.0038$, respectively). The final parameter, number of episodes per droplet, was numerically higher for EMG and EPG head-punctured–wired, though the treatments were significantly different only when the two-sample test of EPG only vs. EMG was performed (d.f. = 1; $F = 19.6$, $P = 0.0010$) (Table 1).

3.3. Comparison of EPG and EMG waveforms using cibarial diaphragm movements

3.3.1. EMG spike bursts and diaphragm movements

In contrast to excretory droplets, EMG spike bursts were strongly correlated with cibarial diaphragm movements, both visually and temporally, as demonstrated both via The Observer video analysis and VMD waveforms. Diaphragm movement waveforms consisted of a rapid rise in voltage followed by a rounded plateau before a steep decline in voltage (Fig. 4b, red waveform). In most cases, the small, negative-going spike that marked the division between sections m and b in the EMG waveform (Fig. 4b, black waveform) occurred at the end of the plateau or during the falling phase (Fig. 4b–g). Insects recorded with both VMD and EMG also showed slow (Fig. 4b), medium (Fig. 4c), and rapid (Fig. 4d) pumping speed within the same individual insect. Regardless of pumping speed, diaphragm uplift was rapid to a nearly maximum height, which was then maintained for a variable period (compare among Fig. 4b–d) before similarly rapid diaphragm release and fall.

EMG spike bursts in relation to cibarial diaphragm movements followed a distinct, but seemingly paradoxical, pattern depending upon pumping speed. At slow speed, the EMG spike burst occurred late in the VMD plateau (Fig. 4b and e), while at medium speed, the spike burst corresponded to the middle of the plateau (Fig. 4c and f). The duration of the spike burst was longer in slow- and medium-speed pumping (about 350 ms). In contrast, the spike burst occurred at the beginning of the plateau during fast pumping, or even during the rise phase up to the plateau (Fig. 4d and g), and the duration of the spike burst was much shorter (175–200 ms). This seeming paradox of muscular contraction occurring at the end of the cibarial diaphragm's rise during slow pumping is described further in Section 4.2.3).

3.3.2. EPG waveform C and diaphragm movements

For all EPG-recorded insects, VMD diaphragm waveforms were similar in appearance (Figs. 6 and 7). In general, the rise of the

Table 1
EPG/EMG-droplets correlation[a]

Mean per insect of:	EPG only	Head-punctured	Head-punctured, wired	EMG only
Time to first droplet (min)	6.9 ± 2.0 a ($n = 7$)	8.1 ± 4.2 a ($n = 7$)	10.3 ± 4.9 a ($n = 7$)	14.3 ± 2.57 a ($n = 7$)
Number of episodes to first droplet	197.9 ± 25.3 a ($n = 7$)	139.4 ± 77.3 a ($n = 7$)	52.4 ± 27.5 a ($n = 7$)	490.9 ± 121.9 b ($n = 7$)
Number of episodes	2626.4 ± 779.8 a ($n = 7$)	1566.7 ± 699.0 a ($n = 7$)	1369.0 ± 555.14 a ($n = 7$)	2557.0 ± 589.5 a ($n = 7$)
Duration of ingestion phase (min)	44.6 ± 14.3 a ($n = 4$)	40.2 ± 13.2 a ($n = 7$)	23.1 ± 6.9 a ($n = 7$)	52.9 ± 4.3 a ($n = 6$)
Number of droplets	1472.5 ± 599.2 a ($n = 4$)	395.4 ± 187.7 b ($n = 7$)	101.4 ± 50.0 b ($n = 7$)	313.0 ± 65.0 b ($n = 6$)
Number of droplets per second (excretion rate)	0.759 ± 0.248 a ($n = 4$)	0.111 ± 0.038 b ($n = 7$)	0.051 ± 0.030 b ($n = 7$)	0.095 ± 0.017 b ($n = 6$)
Number of episodes per droplet	3.6 ± 0.3 a ($n = 7$)	2.9 ± 0.6 a ($n = 6$)	11.1 ± 5.3 a ($n = 7$)	9.1 ± 1.1 a ($n = 7$)

[a] Lower case letters indicate degree of statistical significance among means within each treatment, at $\alpha = 0.05$.

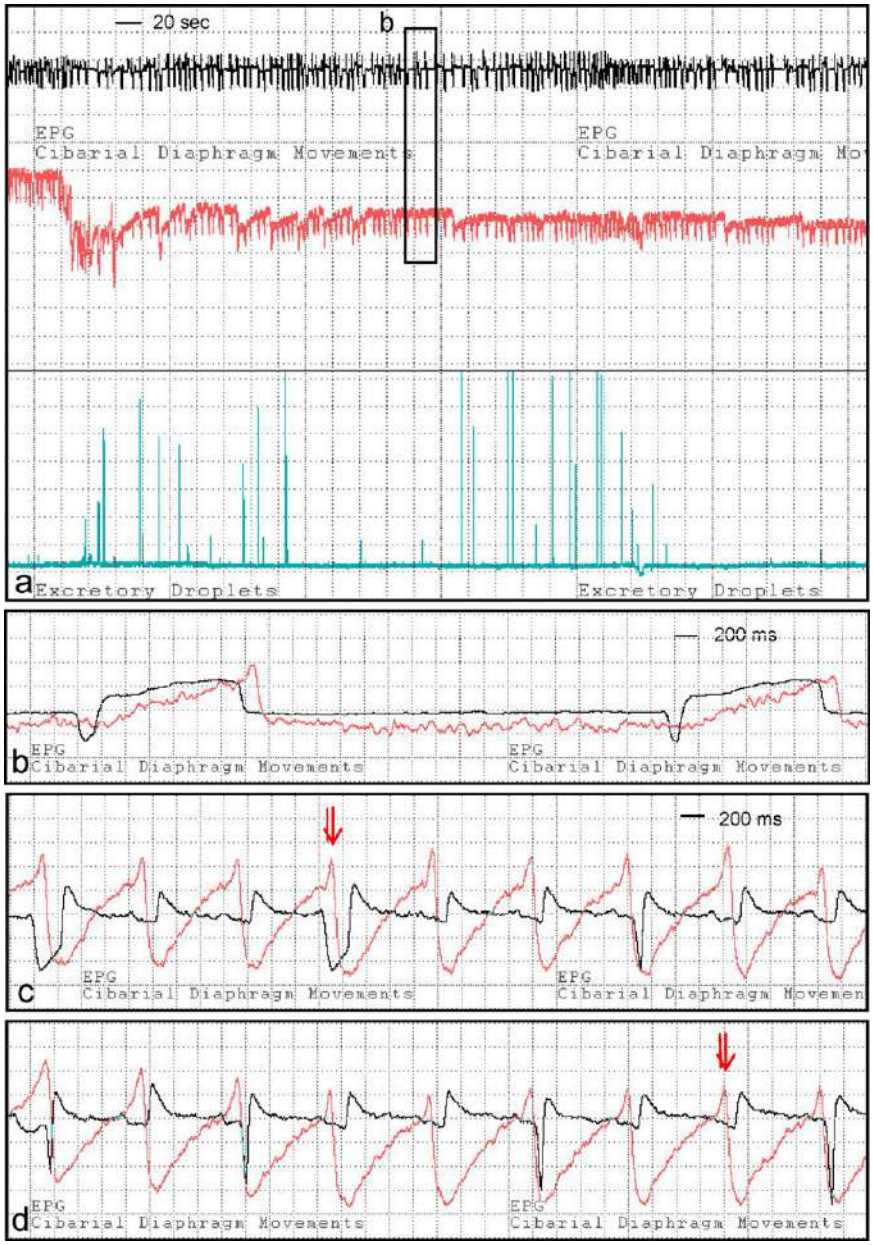

Fig. 6. (a) EPG recordings (black, top channel, user annotation EPG) from a highly wounded, head-punctured–wired control insect, with near-simultaneous VMD recording of cibarial diaphragm movements (red, top channel, user annotation cibarial diaphragm movements). VMD recording of infrequent excretory droplet expulsion (green, bottom channel) is also shown. Same color scheme applies to boxes b, c and d also. Box b is amplified and expanded in part b. WinDaq gain 8× (red and black waveforms), 32× (green waveform). (b) Very slow pumping. Amplification and expansion of box b from part a. WinDaq gain 16×. (c and d) EPG waveforms from unwounded insect (EPG only), showing rapid pumping with frequent loss of full depth of the C valley. Synchronizer lag indicated by red lines and arrows. The red arrow shows the red (VMD) waveform feature that should be moved back to the position of the red line. WinDaq gain 16×. Time scale in part c applies to part d also.

cibarial diaphragm was gradual, reached a peak, then fell rapidly, giving the waveform a triangular appearance (Fig. 6c and d, red lines). The subsequent fall off the C wave plateau into the valley was correlated with the fall in the VMD waveform in medium to slow pumping (Fig. 6b). When the synchronization lag was taken into consideration, the timing of the falling phase of the VMD waveform either matched precisely that of the EPG waveform, or the VMD waveform was slightly ahead in time (Fig. 6c and d, arrows). For both wounded (e.g. EPG head-puncturded, Fig. 6a) and non-wounded insects (i.e. EPG only), the VMD waveform looked different from that of the EMG insects (compare Figs. 4b and 6b–d). The VMD waveform appeared more triangular than rounded, although pumping speed could be either very slow or even near-normal (Fig. 6b–d). We attribute this difference to greater degree of impairment of the cibarial dilator muscles of the EMG insects compared with EPG insects. VMD waveforms for EMG insects were small, requiring greater amplification for Fig. 4 than for Fig. 6. We suspect that less muscular power could be exerted against xylem tension, lending a more rounded shape to the VMD plateaus of EMG insects.

Differences in shape between the EPG and VMD waveforms suggest the interpretation of fluid flow microdynamics detailed in Section 4.2, especially supported in one unique case shown in Fig. 7. This EPG punctured, wired control insect performed medium-speed pumping, often with long inter-pump periods. In addition, this was the only VMD-recorded insect whose body

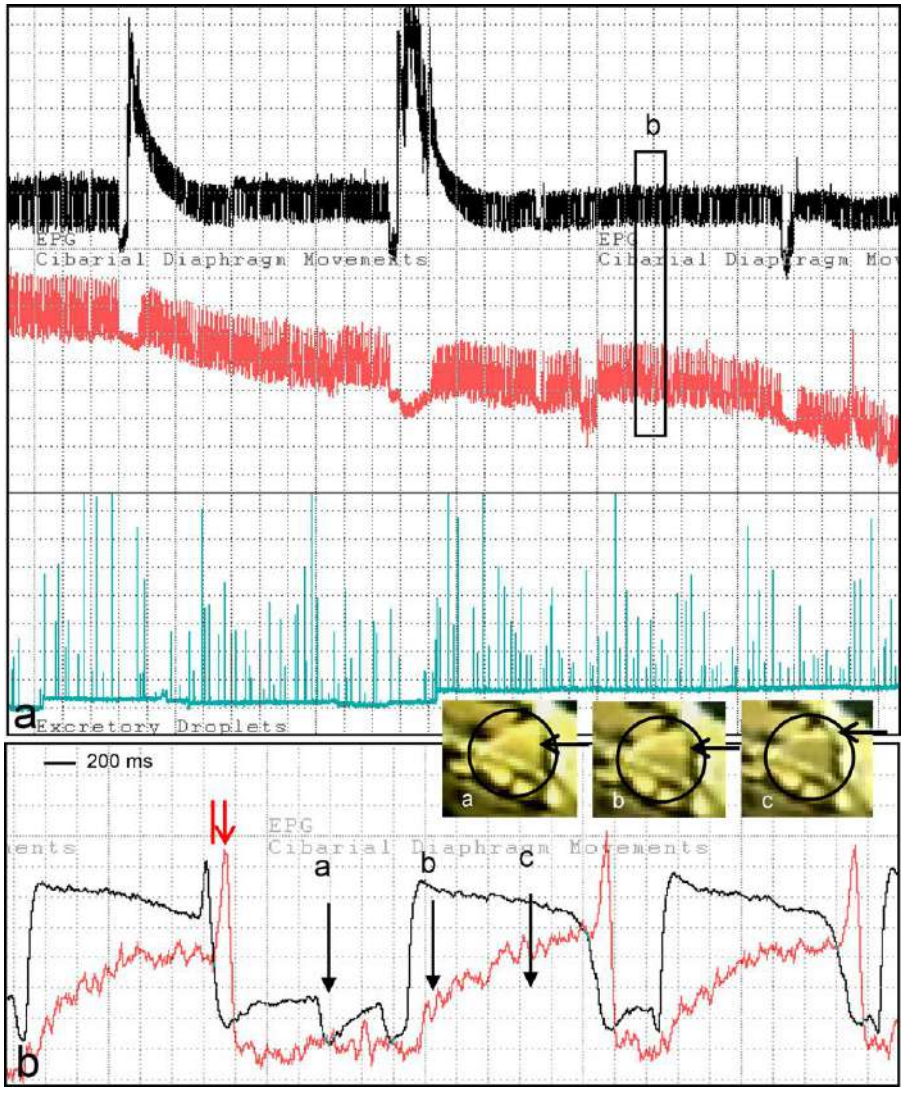

Fig. 7. (a) EPG recordings (black, top channel, user annotation EPG) from a less wounded, head-punctured control insect, with near-simultaneous VMD recording of cibarial diaphragm movements (red, top channel, user annotation cibarial diaphragm movements). VMD recording of more frequent, excretory droplet expulsion (green, bottom channel) is also shown. Same color scheme applies to box b also. Box b is amplified and expanded in part b. WinDaq gain 8× (red and black waveforms), 32× (green waveform). (b) Amplification and expansion of box b from part a. Medium-speed pumping shows complete depth of C valley. Black arrows a, b and c refer to inset boxes a, b and c, showing still images of diaphragm uplift, captured from the video. For an unknown reason, in this case, the backlighting was reversed from usual, so that as the diaphragm raised, the cibarium became darker, and when the diaphragm lowered, it became lighter. Thus, the VMD waveform had to be inverted for this figure, to make it similar in appearance to other VMD waveforms. WinDaq gain 16×. Synchronizer lag indicated by red lines and arrows. The red arrow shows the red (VMD) waveform feature that should be moved back to the position of the red line.

position, by chance, facilitated just the right backlighting to allow the edge of the diaphragm to be visible as it was withdrawn (Fig. 7b, image insets), instead of the more typical, less definitive, light-dark flickering.

The VMD diaphragm waveform represents the physical suction or pressure applied to fluids in the stylets and precibarium, while the EPG waveforms represent the electrical nature of the resulting fluid flow (see Section 4.2.4). The cibarial diaphragm is gradually lifted (Fig. 7b, red line) through a waveform arch that eventually reaches a slight plateau. At the same time, fluid must be gradually sucked inward into the cibarium. Xylem tension is high, probably requiring strong, lengthy suction, and because the large volume of the cibarium (relative to the narrow precibarium) requires time to fill. Electrically, the more rapid rise to the C waveform plateau (Fig. 7b, black line) co-occurs with the rise in the VMD waveform, but much more steeply. The C waveform abruptly rises to a square plateau earlier, and later voltage even declines slightly. At the end of the gradual VMD rise, a sudden spike always occurs (Fig. 7b, red line). Sometimes (more often in some insects than others) there is a simultaneous spike (after accounting for the synchronization lag) at the end of the C waveform plateau as well (Fig. 7b, black line; see also Fig. 5). During this spike, the diaphragm suddenly pulls to its highest point; revealing a slight release of tension as the cibarium is nearly full. Diaphragm release and closure then rapidly occur, as indicated by the voltage valley of the VMD waveform. The similar spike and fall off the C waveform plateau indicates rapid reversal of charges (Fig. 7b).

The fine structure appearance of the EPG waveforms varied more from insect to insect, than did the VMD waveforms (of the EPG-recorded insects). The appearance of the C waveform at Ri $10^6\ \Omega$ was similar to that at Ri $10^9\ \Omega$, except for two interesting differences. First, there was a frequent loss of depth in the C wave

Table 2
Durations (in s) of the EMG or EPG waveform episodes recorded from smoke tree sharpshooters

Recording method	Waveform episode	N	Duration (in sec) ± standard error of the mean[a]
EMG	spikes (p)	1977	0.381 +/- 0.003 a
	middle (m)	824	0.277 +/- 0.002 a
	baseline (b)	1766	0.765 +/- 0.005 b — NSD[b]
EPG	plateau	1070	0.715 +/- 0.005 b
	valley	1004	0.710 +/- 0.030 b

[a]Lower case letters indicate degree of statistical significance among means within each treatment, at $\alpha = 0.05$.
[b]When EMG spikes and middle section durations are added, then compared with EPG plateaus, durations are not significantly different at $\alpha = 0.05$.

valley at Ri 10^6 Ω when pumping was very rapid, compared with the large, quite constant depth when pumping was slow (Figs. 6b and 7) or medium (Fig. 5) or at any pumping speed at Ri 10^9 Ω. For example, in Fig. 5, the waveform shape resembles that at Ri 10^9 Ω (Backus, unpublished data) but the repetition rate is 0.75 Hz, compared with Fig. 6c wherein waveform shape often lacks full valley depth, and the repetition rate is 1.0 Hz. Second, a positive-going peak was occasionally present at the end of the C wave plateau at Ri 10^6 Ω that was strongly correlated with the final, sudden uplift then fall of the cibarial diaphragm.

Notwithstanding these differences among individuals, the C wave plateau was strongly correlated with rising and falling phases of the diaphragm movement triangle (Figs. 4a and 6b–d), and thus, by inference, probably with the EMG spike bursts (section p) plus section m. This visual evidence is further supported by a statistical comparison of EMG and EPG waveforms.

3.3.3. Statistical comparison of EMG and EPG waveforms

The durations of C waveform plateaus and cibarial spike bursts were significantly different according to ANOVA ($F = 18.12$; d.f. = 1, 7; $P = 0.0038$) (Table 2). The mean duration of the cibarial spike burst (p) was significantly shorter than the mean duration of the C plateau ($P = 0.0038$). However, when the duration of section m was added to that of p, the enhanced duration became not significantly different from the C plateau duration ($F = 2.88$; d.f. = 1, 7; $P = 0.1335$). Thus, because the EMG waveform is inferentially linked to the EPG waveform through the VMD waveform, it is likely that the combination of EMG sections p + m correspond with and explain the flat top of the EPG waveform C plateau. The steepest part of the falling phase of the VMD valley and inter-plateau period thus corresponds with section b (baseline) (compare Figs. 4 and 6).

3.4. Summary of results

Our work showed that overall production and duration of sustained trains of excretory droplets clearly reflected and was proportional to overall duration of ingestion. However, neither one single excretory droplet, nor even a set of droplets, was correlated 1:1 with muscular cibarial pumping, nor with fine structure of the EPG ingestion (C) waveform. Statistical results showed that the degree of correlation between EPG/EMG waveforms and excretory droplets depended on the degree of damage to the cibarial dilator muscles. Wounding resulted in longer pumping time, and therefore more EPG/EMG waveform episodes, needed to fill the gut prior to the first excretory droplet. Moreover, wounding caused more episodes to be performed per droplet, fewer droplets per second, and fewer overall droplets to be produced, even though the same overall number of episodes and duration of ingestion were performed. Therefore, excretion could not act as an inferential bridge between EMG and EPG waveforms.

In contrast, cibarial diaphragm movements were specifically, directly, and 1:1 correlated with both EMG cibarial spike bursts and EPG waveform C plateaus. Therefore, cibarial movements provided an excellent inferential bridge between EMG and EPG waveforms, and EPG waveform C represented active cibarial pumping, each plateau representing a single pump of the cibarial dilator muscles. In addition, comparison of the shapes of VMD and EPG waveforms explained directionality of fluid flow through the precibarium and stylets into the cibarium.

4. Discussion

4.1. Comparison of EPG and EMG waveforms using excretory droplets

Different amounts of cibarial pumping were needed to generate a single excretory droplet, correlated with the degree of wounding to the cibarial muscles. Dolezai et al. (2004) show that each excretory droplet of glassy-winged sharpshooter, *H. vitripennis* (slightly larger in size than this study's smoke tree sharpshooter, *H. liturata*) is approximately 2 μl in volume. This presumably is determined by the size of the collecting space on the anal ligulae prior to droplet expulsion. Thus, the greater the degree of wounding, the less fluid is loaded into each standard-sized droplet, because each cibarial contraction/relaxation cycle (i.e. waveform episode) provides a less-strong pull of fluid. More frequent, smaller cycles are needed to collect the same amount of fluid if the muscles are injured.

Consequently, onset of sustained excretion cannot be used as a reliable indicator of onset of ingestion, nor can cessation be used to indicate cessation of ingestion. Logically, and as also discussed in Dolezai (2004), a certain volume of fluid (variable for each insect based on time since last feeding) must be ingested to completely fill the gut before excretion can begin. Once the gut is full, however, our findings show that regular, sustained excretion does indicate near-simultaneous occurrence of regular, sustained ingestion. Accordingly, excretory activity and volume of excreta do provide a rough measure of sharpshooter feeding. However, volumes of excreta collected from feeding sharpshooters are extremely variable (Dolezai et al., 2004). Combined with our findings, this shows that excreta volumes are an inexact proxy for cibarial activity and ingestion behavior. This finding is important for sharpshooter ecologists and vector biologists, whose research findings often rely on this proxy.

Other (non-EPG) electrical methods to measure ingestion, such as use of heartbeat monitors or impedance converters to quantify indirect effects of fluid movement in probed xylem vessels (Dolezai et al., 2004), are more precise than use of excreta volume alone. However, for fine-scale analysis of *X. fastidiosa* acquisition behavior, we have shown that EPG is a more exacting tool.

4.2. Comparison of EPG and EMG waveforms using cibarial diaphragm movements

4.2.1. Appearance of EMG and EPG waveforms

All EMG waveforms resembled typical muscle generator potentials (spike bursts) similar to those recorded in other studies of bare-wire electrodes inserted into insect muscle (e.g. Smith and Menzel, 1989). For EPG, appearance of waveform C in our experiments was identical to waveform C in Backus et al. (2005) (inverted) and Backus and Bennett (not inverted; unpublished data, ms. in preparation) except that our signals were noisier due to the presence of the videocamera inside the Faraday cage. In addition, variability in waveform C fine structure is typical of AC

EPG waveforms (Ri $10^6\ \Omega$) (Almeida and Backus, 2004; Backus et al., 2005), but its biological meaning has been unknown until now.

4.2.2. EMG/EPG correlation

We provide herein the first direct, definitive correlation for any auchemorrhynchan hemipteran of electrically recorded feeding waveforms with cibarial pump cycles, as had previously been shown for *Rhodnius prolixus* Stal (Smith and Friend, 1970), and called for by Smith (1985) in his comprehensive review of insect feeding mechanisms. We also go beyond the work of Smith and Friend (1970) by analyzing the microdynamics of pumping and fluid flow in relation to cibarial diaphragm movements.

Our statistical findings relating EMG and EPG episode durations are strictly correlational, not cause-and-effect. Nonetheless, we propose that the added, inferential bridge of the cibarial diaphragm VMD recordings supports a strong cause-and-effect relationship between the EMG and EPG waveforms. Thus, because EMG sections p + m correspond with the VMD plateau, it is likely that a combination of muscular contraction (section p) and likely cuticular elasticity (section m) is used to elevate the diaphragm. It further follows that because the VMD plateau corresponds with the EPG plateau, then the electrical origin of the EPG waveform is directly influenced by these same muscular and cuticular properties.

Our observational evidence shows that hydrostatic pressure from the cibarial dilator muscles is directly correlated with the EPG ingestion waveform's fine structure. In general, inward cibarial suction is 100% correlated with positive-going EPG voltage changes; outward cibarial pressure is similarly correlated with negative-going voltage changes. The only known electrolytic mechanism that could explain this correlation is streaming potentials, caused by powerful hydrostatic pressures induced by cibarial pumping.

4.2.3. Role of cuticular elasticity in pumping

It is likely that a combination of cuticular elasticity and muscular activity rapidly lifts the cibarial diaphragm during pumping, forming a vacuum in the cibarium that sucks up fluids from the precibarium. Then, when muscle activity ceases, the cibarial diaphragm falls back into the closed position. Because there is no antagonistic muscle set that pulls the diaphragm downward after lift (Backus and McLean, 1983), closure must be accomplished via the elasticity of the cibarial cuticle.

We hypothesize that this cuticular elasticity may act similarly to the click mechanism for insect wing-beats. A harmonically rhythmic "bounce" may develop during cyclic pumping, such that only brief cibarial dilator muscle contractions are needed to maintain very rapid pumping. Slower, more (seemingly) labored pumping by wounded insects probably requires longer muscle contractions to keep the cycle going. Similar to wing-beats, when such a cuticular, click mechanism-like bounce operates, muscular contraction may not always need to precede or power the diaphragm uplift, but merely to occur somewhere in the cycle to keep the bounce going. This explains the seemingly paradoxical occurrence of muscular contractions at the end or middle of the cycle for slow- and medium-speed pumping, respectively. When wounded insects first began cibarial pumping, the pumps were often very slow. Weakened muscles probably required longer pulling time, and could not sufficiently start the upward cuticular bounce to ensure that adequate pressure was exerted against strong xylem tension. Therefore, in wounded insects, after the energy from the elastic bounce dissipated without yet filling the cibarium with fluid, muscular contraction was probably necessary to finish the cycle.

4.2.4. Electrical origin of EPG waveform C fine structure

The new AC–DC EPG monitor used in this study (Backus and Bennett, unpublished data) allows determination of the proportion of electromotive force (emf) vs. resistance (R) components that make up each EPG waveform (Tjallingii, 2000; Walker, 2000) occurring at each Ri level from 10^6 to $10^9\ \Omega$, plus $10^{13}\ \Omega$. Other work in the Backus laboratory has shown that electrical origin of the C waveform at Ri 10^9 and $10^{13}\ \Omega$ is 100% emf, while at Ri $10^6\ \Omega$ the electrical origin of waveform C is a mixture of R- and emf-components (Backus and Bennett, unpublished data; ms. in preparation). For example, the presence of C valley depth during rapid pumping at Ri $10^9\ \Omega$ and its loss at Ri $10^6\ \Omega$ shows that C valley depth is an emf component at that Ri level. Probably emf responsiveness at Ri $10^6\ \Omega$ is not rapid enough to capture the C wave fall when pumping is very rapid. Similarly, the peak at the end of the C plateau is likely to be an R component because it is only seen at Ri $10^6\ \Omega$, a level at which R component features are more visible. Thus, the changes in waveform appearance due to different amplifier sensitivities (to R vs. emf) allowed dissection of C waveform parts by their electrical origins. This, in turn, revealed mechanisms and biological meanings not previously understood.

4.2.5. Mechanisms of emf- and R-components in EPG waveform C

Previous studies have shown that voltages generated within the plant-insect interface (biopotentials) are the primary biological source of emf in EPG signals, and streaming potentials are a prime candidate for emf (Walker, 2000). Walker (2000) describes the mechanism of streaming potentials, and how they might cause EPG waveform fine structure. In summary, when hydrostatic pressure (e.g. from cibarial dilator muscles) generates a flow of electrolyte fluid through a narrow capillary tube (e.g. the stylet food canal and precibarium), physical drag of the fluid plus electrical attraction of the capillary walls cause electrical charges in the fluid to array in a non-uniform fashion across both the diameter and length of the capillary. Thus, a charge difference (voltage) develops between the two ends of the tube (see figure in Walker, 2000). This resulting voltage can increase or decrease (like an AC [alternating current] voltage) based on, among other properties, acceleration of fluid flow in a certain direction. After a brief period of fluid flow, the voltage reaches an electrical equilibrium (i.e. converts to a constant, DC [direct current] voltage), due to the hydrostatic properties of the fluid being counteracted by its electrostatic properties. In other words, once electrical equilibrium is reached, continued physical fluid flow in the same direction no longer generates an AC voltage; it becomes represented by a flat line, or DC voltage. We propose that, at Ri $10^9\ \Omega$, EPG voltage increases (rise to the plateau) or decreases (fall off the plateau) are due primarily to the electrical consequences of initiation of fluid streaming, or reversal in direction, respectively; sustained streaming is represented by an electrically flat line. Thus, fluid is moving anteriorad into the cibarium as the voltage rises to the plateau, and then is pushed posteriorad as the voltage falls off the plateau (probably as swallowing). Our work provides the first direct support for streaming potentials as a mechanism of EPG waveform fine structure, as first suggested by Tjallingii (personal communication) but described in full by Walker (2000).

As already discussed, the EPG peak at the end of the C plateau must be an R component that is due to electrical resistance to fluid flow. We propose that the sudden, abrupt uplift of the cibarial diaphragm, after its slower, more steady rise demonstrated by the triangular VMD waveform, is due to the sudden release of xylem tension against which the muscle/elastic cuticle pressures were pulling. This could only occur if the precibarial

valve, located downstream of the cibarium, were to close suddenly, blocking further fluid uptake (and therefore, electrical conductivity). This probably is the only way that the release and drop of the diaphragm can allow a bolus of fluid food to be swallowed without fluid leaking back into the plant via the stylets (Smith, 1985). The complete blockage of the narrow precibarium for an instant by the precibarial valve probably is a strong resistance component, transduced into a waveform fine structure that is only visible at Ri 10^6 Ω. We further propose that the brief, negative-going EMG spike that demarks the p and m sections of the EMG waveform represents a very brief, muscular closure of the precibarial valve (probably accompanied by some backwash-driven physical lift ["pressure-sensitive check valve"] Backus and McLean, 1982) which occurs at about the same time (using the VMD waveform as an inferential bridge) as the positive-going peak of the EPG plateau. Results from our separate EMG study of precibarial valve movements support this idea (Backus and Dugravot, unpublished data).

4.3. Implications for acquisition and inoculation mechanisms of X. fastidiosa

Inward suction of fluid by *Homalodisca* spp. vectors of *X. fastidiosa* is the major mechanism of bacterial acquisition (Purcell, 1989). Our examination of EPG waveform fine structure in relation to cibarial pumping and fluid dynamics has explained how it is possible for sharpshooters to ingest for many hours from xylem vessels under extreme tension, via a combination of muscular power and cuticular elasticity.

The mechanism of inoculation of *X. fastidiosa* is thought to involve outward flow of fluid from the precibarium to the stylets (Backus and McLean, 1982; Purcell, 1989), presumably carrying bacterial biofilm dislodged from the precibarium and/or cibarium (Almeida and Purcell, 2006). Our work shows that cibarial diaphragm collapse is responsible for the major outward flow of fluid from the cibarium. Our work also suggests that pressure from such outward cibarial flow causes fluid to briefly flow forward into the precibarium, before it is stopped by the precibarial valve, thus allowing the bulk of fluid to be swallowed into the esophagus (Smith, 1985). This further supports the hypothesis that inoculation of *X. fastidiosa* could occur if the precibarial valve fails in its operation, allowing some fluid to leak back into the plant (Smith, 1985). The present work provides a rigorous tool for future studies of inoculation mechanisms, by showing that dynamics and directionality of fluid flow into and out of the foregut can be interpreted from EPG waveform fine structure caused by both streaming potentials and electrical resistance.

Acknowledgments

We thank John Lighton (Sable Systems Inc., Las Vegas, NV) for early discussions of cibarial diaphragm movements. We are indebted to our close colleague, William H. Bennett (University of Missouri, retired) for designing and building the video motion detector, as well as the Synchronizer. As always, we could not do our work without his genius. In addition, we thank Holly Shugart and Jose Gutierrez (ARS Parlier) for rearing insects and plants for this work. Jose Gutierrez also worked assiduously at waveform measurement. We also thank an anonymous reviewer for his substantive and helpful suggestions. This work was supported by a grant from the University of California Pierce's Disease Research Program.

References

Almeida, R., Backus, E.A., 2004. Stylet penetration behaviors of *Graphocephala atropunctata* (Signoret) (Hemiptera, cicadellidae): EPG waveform characterization and quantification. Ann. Entomol. Soc. Am. 97 (4), 838–851.

Almeida, R., Purcell, A.H., 2006. Patterns of *Xylella fastidiosa* colonization on the precibarium of sharpshooter vectors relative to transmission to plants. Ann. Entomol. Soc. Am. 99 (5), 884–890.

Anderson, P.C., Brodbeck, B.V., Mizell III, R.F., 1989. Metabolism of amino acids, organic acids and sugars extracted from the xylem fluid of four host plant by adult *Homalodisca coagulata*. Entomol. Exp. Appl. 50, 149–160.

Backus, E.A., Cline, A.R., Ellersieck, M.R., Serrano, M., 2007. *Lygus hesperus* (Knight) (Hemiptera: Miridae) feeding on cotton: New methods and parameters for analysis of non-sequential EPG data. Ann. Entomol. Soc. Am. 100 (2), 296–310.

Backus, E.A., Devaney, M.J., Bennett, W.H., 2000. Comparison of signal processing circuits among seven AC electronic monitoring systems for their effects on the emf and R components of aphid (Homoptera: Aphididae) waveforms. In: Walker, G.P., Backus, E.A. (Eds.), Principles and Applications of Electronic Monitoring and Other Techniques in the Study of Homopteran Feeding Behavior. Entomological Society of America, Lanham, MD, pp. 102–143.

Backus, E.A., Habibi, J., Yan, F., Ellersieck, M.R., 2005. Stylet penetration by adult *Homalodisca coagulata* on grape: Electrical Penetration Graph waveform characterization, tissue correlation, and possible implications for transmission of *Xylella fastidiosa*. Ann. Entomol. Soc. Am. 98 (6), 787–813.

Backus, E.A., McLean, D.L., 1982. The sensory systems and feeding behavior of leafhoppers. I. The aster leafhopper, *Macrosteles fascifrons* Stål (Homoptera: Cicadellidae). J. Morphol. 172, 361–379.

Backus, E.A., McLean, D.L., 1983. The sensory systems and feeding behavior of leafhoppers. II. A comparison of the sensillar morphologies of several species (Homoptera: Cicadellidae). J. Morphol. 176, 3–14.

Burks, R.A., Redak, R.A., 2003. The identity and reinstatement of *Homalodisca liturata* Ball and *Phera lacerta* Fowler (Hemiptera: Cicadellidae). Proc. Entomol. Soc. Wash. 105 (3), 674–678.

de Leon, J.H., Jones, W.A., Morgan, D.J.W., 2004. Population genetic structure of *Homalodisca coagulata* (Homoptera: Cicadellidae), the vector of the bacterium, *Xylella fastidiosa*, causing Pierce's disease in grapevines. Ann. Entomol. Soc. Am. 97 (4), 809–818.

Dolezai, P., Bextine, B., Dolezalova, R., Miller, T.A., 2004. Novel methods of monitoring the feeding behavior of *Homalodisca coagulata* (Say) (Hemiptera: Cicadellidae). Ann. Entomol. Soc. Am. 97 (5), 2004.

Fry, J.C., 1993. Biological Data Analysis: A Practical Approach. Oxford University Press, Inc., N.Y., N.Y.

Joost, P.H., Backus, E.A., Morgan, D.J.W., Yan, F., 2006. Specific stylet activities by the glassy-winged sharpshooter, *Homalodisca coagulata* (Say), are correlated with AC EPG waveforms. J. Insect Physiol. 52, 327–337.

McLean, D.L., Kinsey, M.G., 1984. The precibarial valve and its role in the feeding behavior of the pea aphid, *Acyrthosiphon pisum*. Bull. Entomol. Soc. Am. 30 (2), 26–31.

Ott, R.L., Longnecker, M., 2001. An Introduction to Statistical Methods and Data Analysis, 5th edition. Duxbury, Pacific Grove, CA.

Purcell, A.H., 1989. Homopteran transmission of xylem-inhabiting bacteria. In: Harris, K.F. (Ed.), Advances in Disease Vector Research. Springer-Verlag, Inc., New York, pp. 243–266.

SAS Institute, 2001. SAS/STAT user's guide, ver. 8.2. SAS Institute, Cary, NC.

Smith, B.H., Menzel, R., 1989. The use of electromyogram recordings to quantify odourant discrimination in the honey bee, *Apis mellifera*. J. Insect. Physiol. 35 (5), 369–375.

Smith, J.J.B., Friend, W.G., 1970. Feeding in *Rhodnius prolixus*: responses to artificial diets as revealed by changes in electrical resistance. J. Insect. Physiol. 16, 1709–1720.

Smith, J.J.B., 1985. Feeding mechanisms. In: Kerkut, G.A., Gilbert, L.I. (Eds.), Comprehensive Insect Physiology, Biochemistry and Pharmacology. Pergamon Press, Oxford, pp. 33–85.

Snodgrass, R.E., 1935. Principles of Insect Morphology. McGraw-Hill Book Co., New York, 667 pp.

Takiya, D., Mckemey, S., Cavichiol, D., 2006. Validity of *Homalodisca* and of *H. vitripennis* as the name for glassy winged sharpshooter (Hemiptera: Cicadellidae: Cicadellinae). Ann. Entomol. Soc. Am. 99 (4), 648–655.

Tjallingii, W.F., 1988. Electrical recording of stylet penetration activities. In: Minks, A.K., Harrewijn, P. (Eds.), Aphids: Their Biology, Natural Enemies and Control. Elsevier, Amsterdam, pp. 95–108.

Tjallingii, W.F., 2000. Comparison of AC and DC systems for electronic monitoring of stylet penetration activities by homopterans. In: Walker, G.P., Backus, E.A. (Eds.), Principles and Applications of Electronic Monitoring and Other Techniques in the Study of Homopteran Feeding Behavior. Entomological Society of America, pp. 41–69.

Walker, G.P., 2000. Beginner's guide to electronic monitoring. In: Walker, G.P., Backus, E.A. (Eds.), Principles and Applications of Electronic Monitoring and Other Techniques in the Study of Homopteran Feeding Behavior. Entomological Society of America, pp. 14–40.

Walker, G.P., Backus, E.A., 2000. Principles and Applications of Electronic Monitoring and Other Techniques in the Study of Homopteran Feeding Behavior. Entomological Society of America, 260 pp.